Self-supporting Functional Nanomembranes of Metal Oxide/Polymer Blends

Anteneh Mersha[1,2(✉)] and Shigenori Fujikawa[3,4]

[1] Department of Industrial Chemistry, Addis Ababa Science and Technology University, Addis Ababa, Ethiopia
`anteneh.kindu@aastu.edu.et`
[2] Nanotechnology Center of Excellence, Addis Ababa Science and Technology University, Addis Ababa, Ethiopia
[3] Graduate School of Engineering, Kyushu University, Fukuoka, Japan
[4] International Institute of Carbon Neutral Energy Research, Kyushu University, Fukuoka, Japan

Abstract. Nanomembranes are important class of nanomaterials, with significantly advancing applications in a wide range of applications, including molecular separations, energy conversion and storage, sensing, catalysis and biomedical applications such as wound dressing, owing to their nano-scale thickness and high aspect ratios. However, in order to exploit the unique features of self-supporting nanomembranes (transferability onto any arbitrary substrate, high aspect ratio and unique interfacial properties), they need to have sufficient macroscopic stabilities. Conventional mechanical enhancement approaches, such as use of nanoparticle fillers often face material compatibility problems, limiting the range of material selection. In this work, a simple one-step strategy for developing functional free-standing nanomembranes (FS-NMs) from blended types of organic/inorganic composites has been presented. Such blending approach offers atomic scale *in-situ* interaction of organic and inorganic structures, ensuring nanoscale stability in membranes. Here, a hydroxyl-terminated polyethylene glycol (PEG-OH) was premixed with different metal oxide precursors for sol-gel assisted membrane formation, and the mechanical properties of the resulting FS-NMs were compared. The gas separation behavior of mechanically stable nanomembranes was also discussed. The presented strategy offers an alternative approach to develop functional self-supporting nanomembranes.

Keywords: Metal oxide · Polymer · Composites · Nanomembranes · Gas separation

1 Introduction

Polymeric films become weak upon thinning to a nanometer-scale and some polymers are difficult to spun into ultrathin films [1], making it unfavorable to prepare purely organic free-standing nanomembranes (FS-NMs). On the other hand, inorganic materials are rigid and fragile to handle as nanomembranes. Organic/inorganic composite materials

combine these conflicting features of polymers and inorganics, and thus, enable the development of mechanically enhanced self-supporting nanomembranes [2].

In addition to incorporation of inorganic fillers into a polymer matrix, composite membranes are prepared by molecular scale integrations such as layer by layer (LBL) assembly [2, 3] and simply blending the organic and inorganic components prior to membrane preparation [4]. This molecular scale approaches enable atomic or molecular level interactions that are essential for the development of mechanically reinforced FS-NMs. Apart from mechanical reinforcement, composite membranes possess higher thermal stability [5], compared to the pristine polymer.

According to Kunitake's group [4], organic/inorganic hybrid interpenetrating networks are interesting pathways to prepare FS-NMs of only a few tens nanometer thickness with large macroscopic size and flexibility. They fabricated nanomembranes from blend formula of the corresponding metal oxide and polymer precursors. However, the membranes were not tested for any applications such as small molecule separation. Similarly, tough hydrogel membranes with micrometer-scale thickness have been developed via non-covalent double network strategy by Gong's [6] and other groups [7] for potential applications such as post-operative antiadhesive and biosensor membranes.

These mechanically robust materials are the motivations to the present work for preparing ultrathin separation membrane employing organic/inorganic hybrid materials. In this work, a metal oxide/polymer hybrid FS-NM was prepared by blending the components prior to membrane fabrication (Fig. 1). Blending approach can offer atomic scale in-situ interaction of organic and ceramic structures in a membrane. We previously reported the preparation of free-standing and ultrathin PVA/TiO_2 composite membrane via LBL assembly [2]. However, despite large lateral size and macroscopic flexibility of the nanomembranes, the CO_2/N_2 separation performance was not satisfactory. In addition to the low CO_2 affinity of PVA, the low separation performance (especially low selectivity) could be associated to pinholes formed either during membrane preparation or processing steps. This, in turn, may come from the hard nature of the nanomembrane where the PVA chain didn't soften the oxide phase sufficiently.

Thus, in addition to changing the membrane architecture, a softer polymer with more CO_2 affinity property was employed aiming to prepare mechanically stable, yet CO_2 selective nanomembrane.
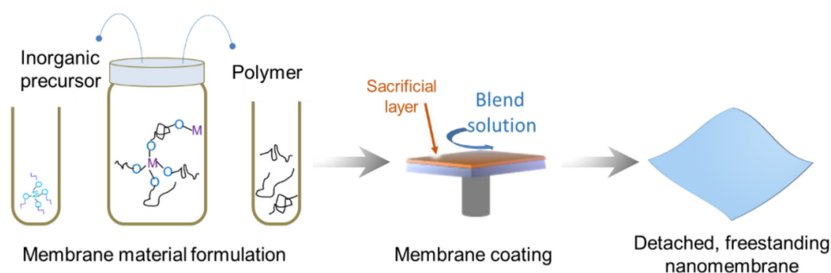
Fig. 1. General representation of hybrid nanomembrane preparation process.

Hydroxyl-terminated polyethylene glycols (PEG-OH) are potential candidates due to their compatibility with metal oxides for sol-gel reactions (Fig. 1), and their CO2 solubility selectivity behavior [8]. Alkoxides are often used as metal oxide precursors. In this study, however, silicon tetraisocyanate was utilized as a source of SiO2 due to its good reactivity, compared to alkoxides. Like alkoxides, the sol-gel reaction involving Si(NCO)4 goes readily to completion as confirmed by previous study [9] (Fig. 2).
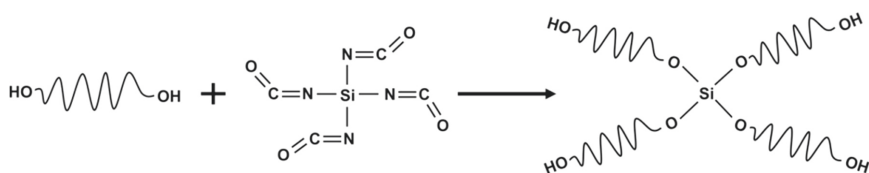
Fig. 2. Scheme for the formulation of organic/inorganic blend material.

In this chapter, the preparation of PEG-OH/SiO$_2$ hybrid nanomembrane with preferential selectivity to CO$_2$ over N$_2$ has been presented. In order to completely avoid gas leakage, a caulking layer of polydimethylsiloxane (PDMS), [10], was employed. To the best of my knowledge, gas permeation properties of such hybrid and free-standing ultrathin membranes have not been studied.

2 Experimental Section

2.1 Materials

Silicon wafer with 350 μm thickness and glass were used as substrates to spin-coat nanomembranes. Poly(4-vinylphenol) (PVP, Mw = 11000, Sigma-Aldrich) was used as a sacrificial layer. Polyethylene glycol (Mw = 2000, Wako Ltd.) was employed as a polymer precursor. Silicon tetraisocyanate (SiNCO)$_4$ (Matsumoto Fine Chemicals Co., Ltd.) and Titanium n-Butoxide (Ti(O^{n}Bu)$_4$, Gelest Inc.) were used as metal oxide precursors. Polydimethylsiloxane (PDMS, Sylgard® 184) was used as caulking material. Ethanol, chloroform and n-hexane were purchased from Wako Co., Ltd. and used as received. Deionized water (18.3 MΩ cm^{-1}, Millipore, Direct-QTM) was used for rinsing and solution preparation.

2.2 Nanomembrane Preparation

In the preliminary step, separate solutions of Si(NCO)$_4$ and PEG-OH were prepared in chloroform, and slowly mixed to prepare blend solutions of PEG-OH and Si(NCO)$_4$ in varying ratios (Table 1). In the meantime, a glass substrate was cleaned by sonication in EtOH for 60 min and subsequent rinsing by deionized water. The glass substrate was dried by air-blowing and treated with oxygen plasma for 4 min to hydrophilize its surface. The oxygen plasma treatment is described elsewhere [2]. Afterwards, a PVP (15 wt%, in EtOH) sacrificial layer was spin-coated (3000 rpm, 60 s) on the glass substrate and heated at 120 °C for 5 min.

Table 1. PEG-OH and Si(NCO)$_4$ ratio optimization from the view point of reactive sites and membrane formation tendency.

S/N		1	2	3	4	5	6
Molar ratio (PEG-OH/SiO$_2$)		9:1	4:1	2:1	1:1	1:2	1:4
Concentration (Total=400mM)	PEG-OH	360	320	268	200	132	80
	SiO$_2$	40	80	132	200	268	320

Once cooled down to room temperature, a PEG-OH/SiO$_2$ blend solution was deposited on the pre-coated sacrificial layer at 3000 rpm for 2 min, and heated at 100 ℃ for 12 h. For membranes to be used in gas permeation test, a 10 wt% PDMS caulking layer was spin-coated. Finally, the glass substrate was immersed in ethanol to dissolve the sacrificial layer and release the free-standing nanomembrane. The overall membrane preparation process is illustrated schematically in Fig. 3.
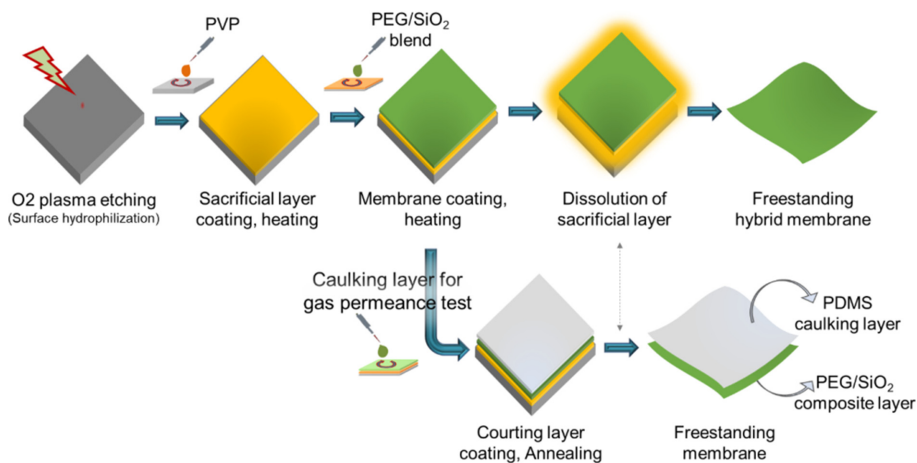
Fig. 3. Schematic representation of nanomembrane fabrication process by spin-coating.

Film thickness and surface morphology were investigated by scanning electron microscope (SEM, Hitachi S-5200). Specimen for surface observation was prepared by transferring the nanomembrane onto supports such as anodized porous alumina (Anodisc, G.E. Healthcare).

2.3   Gas Permeation Experiment

For gas permeation test, the prepared nanomembranes were transferred onto a porous polyimide support. After transfer onto a porous support, membrane area (space through which gas molecules pass) was limited by Kapton tape with the open hole of 1 cm diameter as illustrated in our previous work [2].

Subsequently, the membrane was placed in a home-made membrane cell, and gas permeation was measured using a bubble flow meter (Fig. 4). The pure gas flow rate in cm^3/min of CO_2 and N_2 was measured and converted into permeance (P) using the following equation. Selectivity (α) was also determined as the ratio of permeance.

$$P = \frac{N}{A \cdot \Delta P} \tag{1}$$

$$\alpha = \frac{P_{CO2}}{P_{N2}} \tag{2}$$

where N (m^3/s) refers to the flow rate measured on the permeate side, A (m^2) is effective membrane area and ΔP (Pa) is pressure difference between the feed and permeate side. In the experiment, effective area of gas permeation was 0.785 cm^2. For convenience, permeance was reflected in the common GPU unit, where $1 GPU = 7.5 \times 10^{-12}$ m^3/m^2·s·Pa, at standard temperature and pressure conditions.
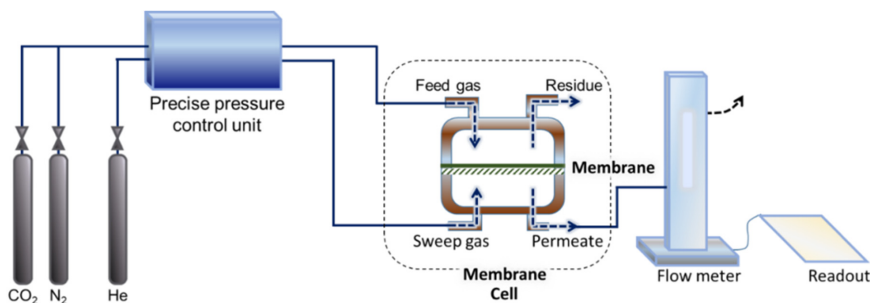

Fig. 4. Single gas permeation measurement apparatus.

The flow rate of CO_2 and N_2 was measured separately and transformed into permeance. Helium was used as a sweep gas in both cases. The feed gas volume and pressure conditions were set at 100 sccm and 0.2 MPa, respectively.

3   Results and Discussion

3.1   Membrane Material Selection and Preparation Conditions

In preparing a blend solution, suitable mixing ratio of the polymer and metal oxide (MO_x) precursor was very important for homogenous distribution of organic and inorganic structures. The PEG-OH/SiO$_2$ ratio was determined based on the sol-gel reactive

sites of the PEG-OH and MO_x precursor; i.e., the number of OH-groups per mole of PEG was measured and converted into -OH and the number of NCO-groups in $Si(NCO)_4$. PEG-OH has two reactive sites and $Si(NCO)_4$ has four reactive sites per mole. Thus, stoichiometrically, 2 mol of PEG-OH react with 1 mol of $Si(NCO)_4$, i.e., PEG-OH/$Si(NCO)_4$ ratio of 2:1.

Based on this, wide range of ratios were prepared and evaluated for their film formation behavior. The result is summarized in Table 2. Also, the effect of temperature on membrane formation and stability was studied. Films were annealed at 100 ºC to facilitate the sol-gel reaction.

Table 2. PEG-$(OH)_2$/$Si(NCO)_4$ ratio optimization from the viewpoint of membrane formation behavior.

| Annealing condition	PEG-$(OH)_2$/$Si(NCO)_4$ ratio*					
	9:1	4:1	2:1	1:1	1:2	1:4
Ambient, 12hrs	No film		Film formed, but fragile		Solution was not stable for film preparation (Fast hydrolysis)	
100 ºC, 12 hrs	Non-detachable film		Stable free-standing film			

*Molar ratio; PEG-OH : $Si(NCO)_4$

As can be seen in Fig. 5 and Table 2, there was an obvious enhancement in the chemical and mechanical stabilities of the prepared nanomembranes after thermal treatment, compared to ambient condition. This should be because heating facilitated the sol-gel crosslinking reaction. Accordingly, stable free-standing PEG-OH/SiO_2 hybrid nanomembranes were obtained from thermally annealed 2-to-1 and 1-to-1 combination of PEG-OH/$Si(NCO)_4$. The membranes maintained their shape and size after detachment from substrates.

3.2 Morphological and Mechanical Properties

In addition to blending ratio and annealing temperature, it is worth explaining that the reactivity of the MO_x precursor affects the membrane formation and subsequent mechanical properties. As discussed in our previous work [2], $Ti(O^nBu)_4$ was used as a MO_x precursor to prepare PVA/TiO_2 composite nanomembrane. However, when replacing PVA by polyethylene glycol (for its softer nature and CO_2 affinity property) to make PEG-OH/TiO_2 nanomembranes, the membranes became more fragile, even under heating at 70 ºC for 12 h. The appearance of the nanomembranes is shown in Fig. 6. Although the annealing temperature of PEG-OH/TiO_2 (70 ºC) was milder than that of PEG-OH/SiO_2 case (100 ºC), the main reason for film fragility could be attributed
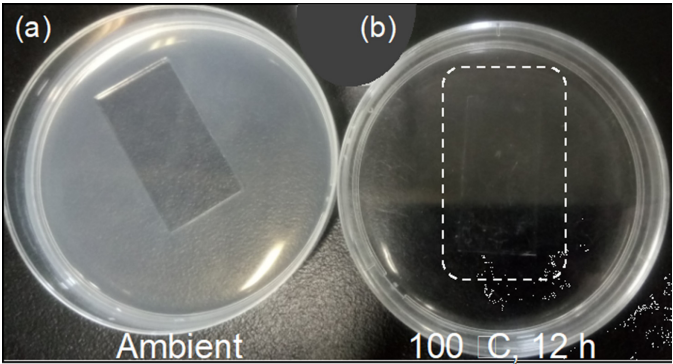
Fig. 5. Digital images showing the difference in the stability of the PEG-OH/Si(NCO)$_4$ films during immersion in EtOH for detachment. (a) PEG-OH/Si(NCO)$_4$ film directly immersed in EtOH. The murky appearance of the solution indicates the dissolution of membrane components. (b) PEG-OH/Si(NCO)$_4$ film immersed in EtOH after annealing at 100 °C. Solution remained clear implying that no new species was introduced into the solvent, except the PVP sacrificial layer.

to lesser sol-gel reactivity of PEG-OH relative to PVA. Apparently, this could be due to lesser proportion of -OH groups in PEG-OH than PVA. Therefore, Si(NCO)$_4$ was tested instead of Ti(O^{n}Bu)$_4$ as a MO$_x$ precursor to compensate the milder reactivity of PEG-OH.
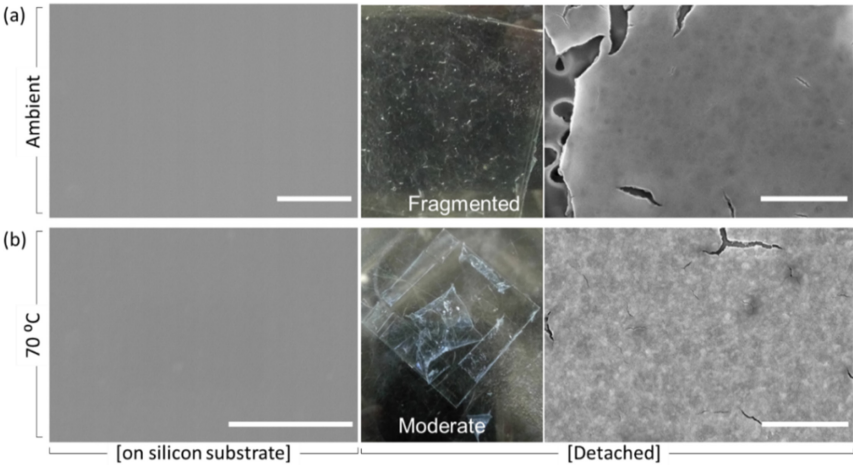

Fig. 6. Nature of PEG-OH/TiO$_2$ hybrid nanofilm under ambient condition (a) and annealing at 70 °C for 12 h (b). **Scale bar: 1 μm**.

Interestingly, a better integrity with PEG-OH has been observed, leading to the realization of large size (Fig. 7a), stable nanomembrane that can be detached and trans-ferred onto a porous support without significant damage. As mentioned above, thermally

annealed 2-to-1 and 1-to-1 molar ratios of PEG-OH/Si(NCO)$_4$ could form large size nanomembranes.

However, despite successful preparation of large size PEG-based nanomembrane, cracks were observed under SEM (Fig. 7b,c). It was seen from physical manipulation and SEM observation that the PEG-OH/SiO$_2$ nanomembrane showed rigid behavior. Although the mechanical property of this membrane was not pleasing, we considered evaluating its gas separation property as a proof of design concept.
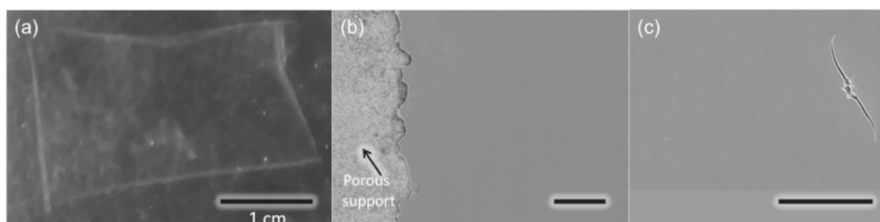
Fig. 7. (a) Digital image of the PEG-OH/SiO$_2$ nanomembrane while it was in the detachment solvent. (b,c) SEM image of the nanomembrane transferred onto a porous support. **Scale bar: 10 μm**.

3.3 Gas Permeation Property

Upon testing the gas permeation, the bare PEG-OH/SiO$_2$ membrane showed frequent gas leakage problem. On the other hand, although not consistently reproducible, the membrane randomly showed CO$_2$ selective separation behavior over N$_2$. In situations like this, a caulking layer is applied to alleviate the effects of structural defects [10]. Caulking materials need to have high gas diffusivities, so as not to hinder the performance of the separation layer. Accordingly, a PDMS caulking layer has been coated on PEG-OH/SiO$_2$ (Fig. 8) in order to seal the cracks and prevent simple gas leakage.
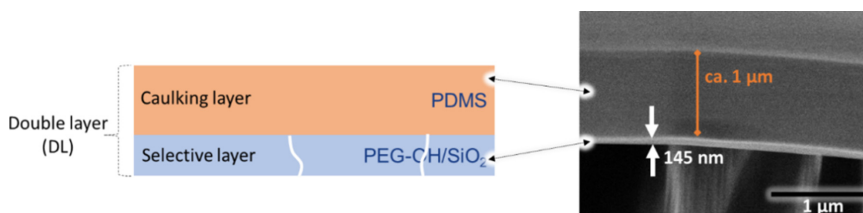
Fig. 8. Schematics (left) and cross-sectional SEM view (right) of PEG-OH/SiO$_2$ nanomembrane with PDMS caulking layer.

From the permeance and selectivity results in Table 3, the CO$_2$/N$_2$ selectivity of (PEG-OH/SiO$_2$)/PDMS membrane was approximated as ca. 15. This value is higher than the CO$_2$/N$_2$ selectivity of pristine PDMS (11.6) [11], signifying that the enhanced

selectivity is due to PEG-OH/SiO_2. This is reasonable as the ethylene oxide group in PEG-OH could assist the solubility-selectivity of CO_2 over N_2. However, the improved CO_2/N_2 selectivity was compromised by a decrease in permeance relative to pristine PDMS. This might be because the PEG-OH/SiO_2 layer was very dense and had no molecular pathways. This, in turn, could be attributed to the presence of amorphous SiO_2 in the membrane, as well as the crystalizing nature of PEG [12] that restricts permeation pathways.

Table 3. Gas separation properties of pristine PDMS and PEG-OH/SiO_2 with PDMS caulking layer.

Membrane	Permeance, GPU		CO_2/N_2 selectivity
	CO_2	N_2	
Pristine PDMS	3500.00	301.000	11.6
PEG-OH/SiO_2 (with caulking layer)	5.50	0.370	14.8
PEG-OH/SiO_2 layer (Resistance model calculation)	5.52	0.371	14.9

The effect of the caulking layer on gas separation behavior of PEG-OH/SiO_2 was examined by applying the resistance model [10, 13, 14]. According to the model, the permeance of the double layer (P_{DL}) membrane is related to the permeance of each layer as follows;

$$\frac{1}{P_{DL}} = \frac{1}{P_{PDMS}} + \frac{1}{P_{PS}}$$ (3)

where, P_{PDMS} and P_{PS} are the permeances of PDMS caulking layer and PEG-OH/SiO_2 selective layer, respectively.

This relation is valid only when the two layers are free of any defects. The PEG-OH/SiO_2 layer, however, possessed cracks (Fig. 7c), meaning that small part of the PDMS layer is not in contact with PEG-OH/SiO_2. Therefore, the experimentally measured permeance (P_{meas}) is not equal to P_{DL}, [14], but rather they are related as follows.

$$P_{meas} = P_{DL}\frac{A_{PS}}{A_{PDMS}} + P_{PDMS}\left(1 - \frac{A_{PS}}{A_{PDMS}}\right)$$ (4)

where, the A_{PS}/A_{PDMS} refers to the area of the PEG-OH/SiO_2 layer covered by PDMS.

It is assumed (based on SEM observation) that the cracks in the PEG-OH/SiO$_2$ layer constitute about 5% and the rest 95% of the membrane was covered by PDMS. The calculated permeance and selectivity values are listed in Table 3. However, there was no significant difference between the experimentally measured and model-based calculated values. This means that the caulking layer has almost no resistance on gas permeation, and the results reflect the behavior of PEG-OH/SiO$_2$ layer. This, in turn, affirms that the PEG-OH/SiO$_2$ nanolayer has no serious cracks.

4   Discussion

The idea of PEG-OH/TiO$_2$ and PEG-OH/SiO$_2$ blend nanomembranes discussed in this paper was a follow up work of PVA/TiO$_2$ LBL nanomembrane discussed presented elsewhere, [2], with the aim to find out an alternative preparation route to integrate macroscopic mechanical property with CO$_2$/N$_2$ separation function.

Two possible ways were considered in order to overcome the low separation performance (where unsatisfactory mechanical stability could be a likely factor) of the PVA/TiO$_2$ nanomembrane; using a softer polymer with better gas separation properties, and changing the membrane architecture. Accordingly, a blended type of PEG-OH/SiO$_2$ FS-NM was developed from a blend formula of a hydroxyl-terminated polyethylene glycol (PEG-OH) and silicon tetraisocyanate. Although no significant mechanical property enhancement was seen, compared to the PVA/TiO$_2$ membrane, the PEG/SiO$_2$ hybrid nanomembrane demonstrated improved CO$_2$/N$_2$ selectivity.

5   Conclusion

Free-standing PEG-OH/SiO$_2$ blend nanomembranes were prepared by spin-coating. The sol-gel reaction between PEG-OH and Si(NCO)$_4$ was assisted by thermal annealing for improved mechanical property. Because the bare composite nanomembrane showed gas leakage due to cracks, PDMS caulking layer has been introduced and the gas separation property was estimated by employing the resistance model. Although no significant mechanical property enhancement was observed from physical manipulation, compared to the PVA/TiO$_2$ LBL nanomembrane discussed in our previous report, [2], the PEG-OH/SiO$_2$ hybrid nanomembrane demonstrated improved CO$_2$/N$_2$ selectivity.

References

1. Koros, W.J.: Macromol. Symp. **188**(1), 13–22 (2002)
2. Mersha, A., Selyanchyn, R., Fujikawa, S.: CleanE **1**(1), 80–89 (2017)
3. Richardson, J.J., Bjornmalm, M., Caruso, F.: Science **348**(6233), 2491 (2015)
4. Vendamme, R., Onoue, S.-Y., Nakao, A., Kunitake, T.: Nat. Mater. **5**(6), 494–501 (2006)
5. Xu, Z.L., Yu, L.Y., Han, L.F.: Front. Chem. Eng. China **3**(3), 318–329 (2009)
6. Ye, Y.N., et al.: Adv. Funct. Mater. **28**(31), 1801489 (2018)
7. Fei, R., Means, A.K., Abraham, A.A., Locke, A.K., Coté, G.L., Grunlan, M.: Macromol. Mater. Eng. **301**(8), 935–943 (2016)
8. Liu, J., Hou, X., Park, H.B., Lin, H.: Chem. Eur. J. **22**(45), 15980–15990 (2016)

9. Takaki, R., Takemoto, H., Fujikawa, S., Toyoki, K.: Colloids surfaces a physicochem. Eng. Asp. **321**, 227–232 (2008)
10. Dal-Cin, M.M., Darcovich, K., Saimani, S., Kumar, A.J.: Memb. Sci. **361**, 176–181 (2010)
11. Robb, W.L.: Ann. N. Y. Acad. Sci. **146**, 119–137 (1968)
12. Lin, H., Freeman, B.D.: Macromolecules **39**(10), 3568–3580 (2006)
13. Henis, J.M.S., Tripodi, M.K.J.: Memb. Sci. **8**(3), 233–246 (1981)
14. Ai, M., et al.: Carbon Nanomembranes (CNMs) supported by poly-mer: mechanics and gas permeation. J. Adv. Mater. **26**(21), 3421–3426 (2014)